

# Guidance on the design and use of fibre-reinforced polymer (FRP) soil nails and ground anchors



**Frans van der Merwe PrEng**  
Principal Geotechnical Engineer  
GaGE Consulting  
frans@gageconsulting.co.za



**Pierre Hofmann**  
General Manager: Geotechnical Product Line  
Dextra (based in Guangdong)  
phofmann@dextragroup.com

*We do not fear the unknown.  
We fear what we think we  
know about the unknown.*  
– Teal Swan

Glass fibre reinforced polymer (GFRP) has been used in many applications in engineering and civil engineering. These materials were first developed and used in the 1930s in the USA in boats and in aeronautical fields. Glass fibre reinforced polymer (GFRP) bars have high strengths, are light in weight, flexible and can be produced more cheaply than carbon fibre. They are also more durable than steel, as they do not corrode. Figure 1 shows a construction worker carrying GFRP soil nails for the MTR Shatin Central Link in Hong Kong. FRP has been used in mining and tunnelling for many years and is now being used in soil nails and tieback ground anchor applications due to the durability concerns associated with conventional steel reinforcement.

No guidelines could be found that assist the designer of soil-nailed retaining structures in the use of FRP bars. This article therefore aims to combine various sources and provide guidance on the design of lateral support systems using FRP bars as soil nails or ground anchors.



**Figure 1** MTR Shatin Central Link, Hong Kong

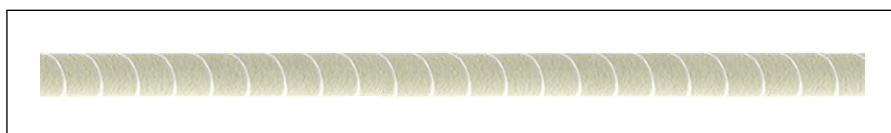


**Figure 2** Dextra GFRP rebar with FRP fibres wrapped around the longitudinal bar together with sand coating to enhance bond strength

It is well known that steel soil nails are normally designed for tension only, although shear forces and associated bending moments might develop at the interface with the failure plane. FRP is normally considered to have small shear capacities and therefore shear forces might influence the performance when they are used in a soil nail application.

## **CURRENT PRACTICE IN THE DESIGN OF SOIL-NAILED WALLS AND ANCHORED RETAINING STRUCTURES**

Current practice in southern Africa for soil-nailed or multi-anchored embedded retaining walls includes the use of either

high-yield threadbar, self-drilling anchors (SDA) or multiwire high-tensile steel strands. These elements, when used in a permanent scenario, require significant corrosion prevention measures. Often high-yield threadbar and SDAs are designed using a sacrificial corrosion thickness allowance. This is highly questionable over the couplers applied to SDAs and when read in conjunction with international codes of practice.

The performance of a steel soil nail is normally assessed by evaluating its unidirectional tensile capacity, and simple empirical calculation methods (wedge analysis or triangular resultant earth pressure).

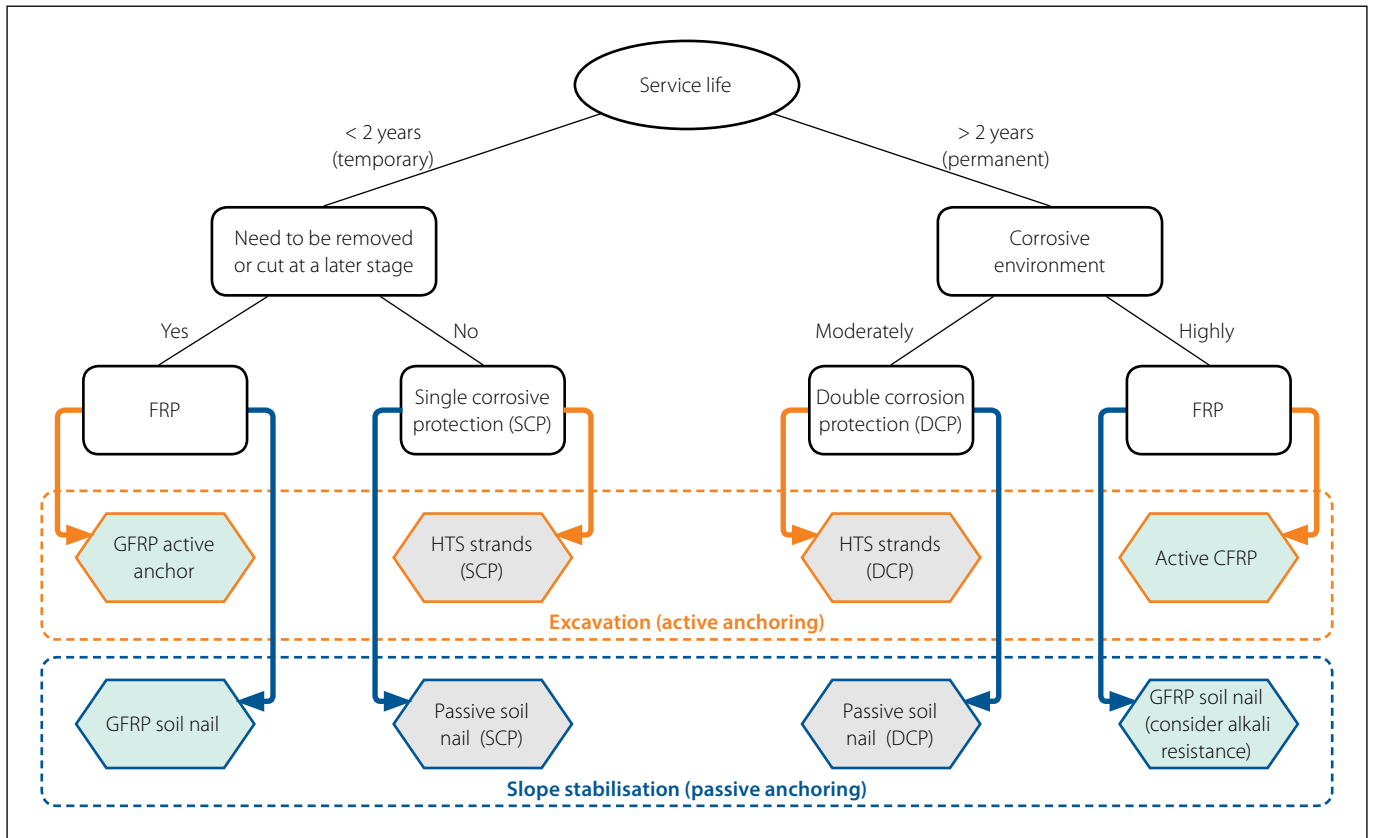


**Figure 3** Reinforcement selection based on corrosive environment

Although these elements also experience shear forces and bending moments where they intersect with the shear plane, these checks are generally disregarded, as it is considered that steel reinforcement in combination with grout is much stronger than the shear force and bending moment requirements. These structural forces can, however, be assessed by using geotechnical finite element packages.

Glass fibre reinforced polymer (GFRP) and carbon fibre reinforced polymer (CFRP) are durable elements but come with other complications, such as long-term creep (similar to geosynthetic materials), susceptibility to alkali attack, temperature variations and ultraviolet light exposure, and reduced shear capacity. Fibre-reinforced bars are anisotropic in nature and are manufactured by a pultrusion process embedded in either a polyester, vinylester or epoxy resin matrix, and therefore have a high tensile strength in the longitudinal direction. These resins are designed to transfer load between the fibres that provide the required strength. CIRIA (2005) states that polyester resin provides good mechanical resistance and electrical properties with reasonable chemical resistance. Epoxy resin provides better resistance to alkalis and solvents with slightly less weathering resistance. Vinylester

together with electrical and chemical resistant (ECR) glass is often the chosen resin and fibre combination due to its ability to resist degradation. One of the main concerns about the performance of FRP is the potential to degrade in the long term in the high-pH environment of the grout body itself. Steel, in comparison, is isotropic in nature. The shear and bond capacity and the thread of bars can be controlled by the addition of FRP fibres wrapped at 45° to the longitudinal direction (Cheng *et al* 2009), as shown in Figure 2. GFRP is more economical than CFRP (twice the price of conventional strand anchors) and will typically be the preferred option from a cost perspective, despite CFRP having superior stiffness and creep performance properties. In active application (stressed ground anchors), however, CFRP is the preferred choice, as will be discussed under *Mechanical Behaviour* later in this article. GFRP and CFRP weigh roughly 20 and 25% of steel respectively.

### RECOMMENDED PRACTICE

The current SAICE Lateral Support to Surface Excavation Code of Practice (1989) recommends the use of double corrosion protection (DCP) in permanent applications, although many practitioners rather use sacrificial thickness design methods

on soil nails. It appears from a review of international standards that, when working in a highly aggressive environment, DCP needs to be used to ensure the lifespan of steel soil nails. The selection tree in Figure 3 is provided to assess when FRP would be advantageous to a project in comparison with steel elements, and shows that in a highly corrosive environment FRP will be the preferred solution. In addition, when the reinforcement needs to be cut by a TBM or piling rig, FRP is ideal.

### MECHANICAL BEHAVIOUR

Figure 4 shows the stress-strain behaviour of various FRPs compared with steel. It can be seen that FRPs are generally much stronger, with a higher ultimate strength for bars of the same diameter when compared with conventional steel reinforcement.

CFRP exhibits slightly lower elastic moduli (66–100%) compared with steel, while GFRP exhibits much lower elastic moduli when compared with steel (20–25% of steel). ASTEC GFRP has elastic moduli of up to 60 GPa.

Tables 1 and 2 are provided to compare the design and working tensile load capacity derived in accordance with ACI440 (2015 and 2022 (to be released)) for GFRP solid bars and SANS 10162 for high-yield

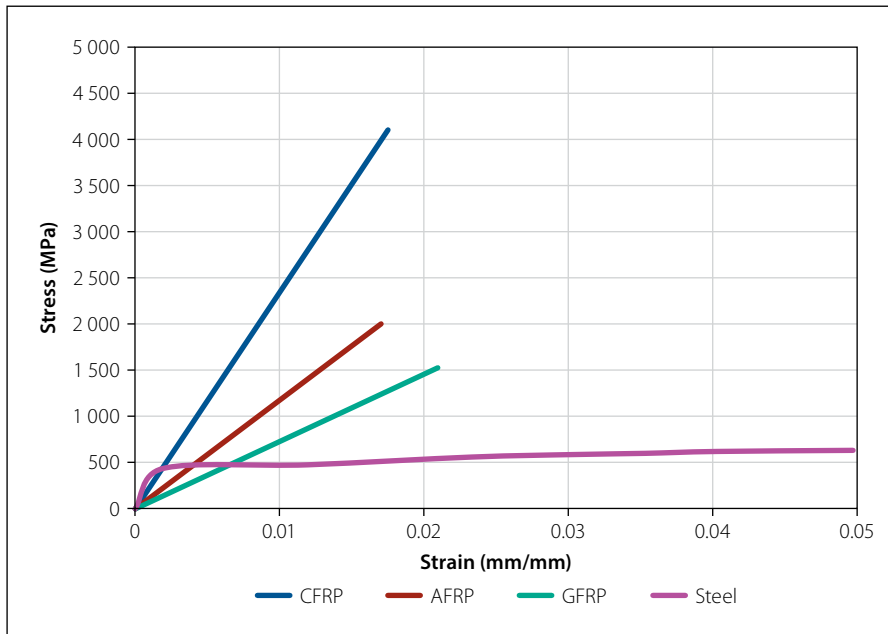


**Figure 4** Stress-strain properties of GFRP, CFRP and conventional steel

threadbar. GFRP also comes in hollow bar sections that can be used as self-drilling anchors (SDA) in collapsible profiles.

From these tables it can be established that, although GFRP is considerably stronger than steel, depending on its manufacturing process, the factored design capacities are much smaller. This can be attributed to the creep properties of the FRP bars. Thomas (2019) states that the working load for a GFRP and steel bolt (assumed to be a high-yield threadbar) is the same, and that a steel bar can therefore typically be replaced by a GFRP bar of the same diameter. However, the tables show that, typically, use of a GFRP might require a bar slightly larger in diameter than a high-yield threadbar to ensure that the same tensile load can be achieved under working load conditions (SLS),

**Table 1** Design ultimate tensile loads and working tensile loads of GFRP

GFRP bar diameter (mm)	Unfactored ultimate tensile load (kN)	Design ultimate tensile load (kN)	Working tensile capacity (kN) ACI440 (2015/2022) at 100 years	Axial stiffness EA (MPa.m <sup>2</sup> )
19	300	114	42/62	14
25	428	161	60/89	24
32	631	239	88/132	40
41	990	375	138/207	66

**Table 2** Design ultimate tensile loads and working tensile loads of high-yield threadbar

High-yield threadbar	Unfactored ultimate tensile load (kN)	Design ultimate tensile load (kN)	Working tensile capacity (kN)	Axial stiffness EA (MPa.m <sup>2</sup> )
20	172	110	73	62
25	269	172	114	98
32	442	281	187	160
40	691	440	293	251

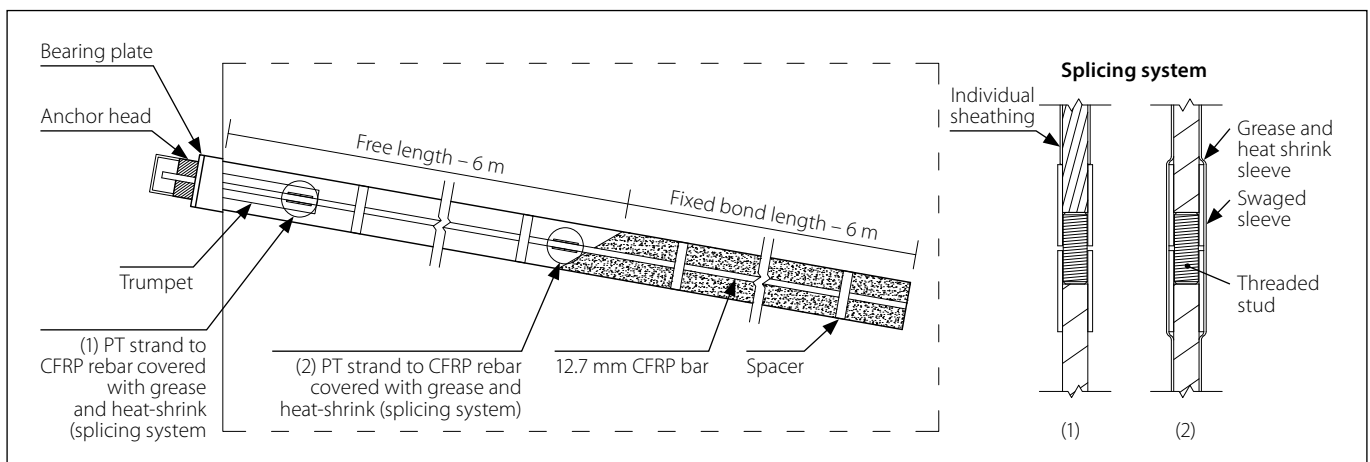


**Figure 5** Prestressed CFRP rods

**Table 3** Design ultimate tensile loads and working tensile loads of both HTS strands and GFRP strands

Strand/bar	Unfactored ultimate tensile load (kN)	Design ultimate tensile load (kN)	Tensile capacity (kN) at 2 years	Working tensile capacity (kN) at 100 years	Axial stiffness EA (MPa.m <sup>2</sup> )
15.2 (HTS low-relaxation strand)	260	210	168	140	36
19 (GFRP)	300	114	100*	42	14
12.7 (CFRP)	250	123		123	16

\* Below 30% unfactored ultimate tensile load to prevent significant relaxation and increased displacement of embedded retaining wall

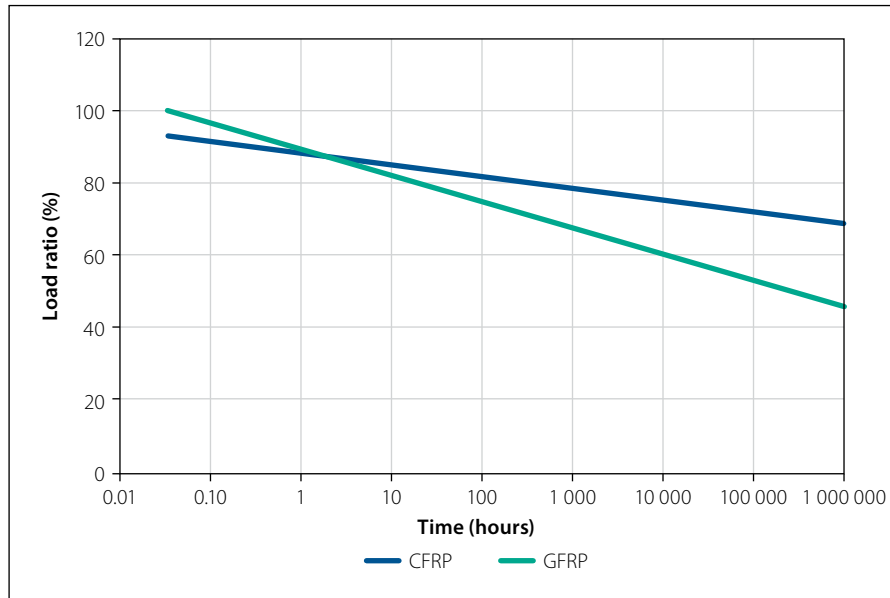


**Figure 6** Creep rupture curves for GFRP and CFRP

which will be most critical for FRP when considering ACI440 (2022).

The axial stiffness of a GFRP bar, even with an increase in diameter, is still lower than that of a high-yield threadbar of one size smaller. The different material properties indicate that larger deformation should occur in a GFRP soil-nail wall compared with a soil-nail wall reinforced with high-yield threadbar. No case studies could be found to prove this.

GFRP or CFRP can also be used to replace HTS stressed tiebacks which might cause significant problems in a permanent scenario with double corrosion protection requirements. It should, however, be remembered that ground anchors are typically made of high-tensile steel (3 to 4 times stronger than conventional steel) and that this plays a major role in determining the number of “equivalent” GFRP or CFRP bars. Typical CFRP anchor configuration details are provided in Figure 5. The CFRP is spliced with a swaged sleeve and threaded stud, as shown in the figure.

Table 3 compares the conventional 15.2 mm HTS low-relaxation strand with a 19 mm GFRP rod. The table shows that

3 × 19 mm GFRP bars may be required to replace one 15.2 mm HTS strand effectively for a long-term (100-year) application. This also implies that the combined axial stiffness will be larger than that of one 15.2 mm HTS strand, and that smaller additional deflection could result with additional load attracted during excavation in a multi-anchored piled wall. Also, a larger-diameter borehole will be required to house the additional number of GFRP bars, but a larger diameter will result in an increased bond resistance. Today, however, it is standard practice to only use CFRP bars in permanent active applications (stressed ground anchors), as the differences between HTS and CFRP are less pronounced. The significant reduction in short-term ultimate strength can be attributed to the long-term creep

behaviour of GFRP bars, which is similar to that of geogrids.

Conventionally, for geogrids in the serviceability limit state, the time-dependent constant tensile force-versus-strain behaviour, at various magnitudes of working loads, is very important. This is normally reported as an isochronous curve, and a post-construction strain limit of 0.5–1.0% for MSEW structures governs the SLS. If an additional strain from post-construction of 1% occurs on an 8 m free length, additional movement of 80 mm can occur. This would be detrimental to the behaviour of an embedded retaining wall and therefore the aim is to design for close to 0% post-construction strain with GFRP and CFRP.

Although it does not seem to be common practice to provide isochronous curves, or plots of creep strain versus time at various stress levels for particular fibre reinforced bars as detailed in ACI440, this is considered crucial to assess.

Youssef and Benmokrane (2014) undertook creep tests on six commercially available GFRP bars in Canada, at tensile loads of 15 and 30% of the ultimate tensile strength. These tensile force ratios are close to the SLS tensile capacity derived in Tables 1–3, and are in accordance with ACI440. The bars loaded to 15% of the short-term ultimate tensile strength had almost no creep during the constant load test, while the bars stressed to 30% crept slightly, but within acceptable limits, with time.

The creep rupture of GFRP and CFRP is important for the ULS design strength and is provided in Figure 6. The figure

*The axial stiffness of a GFRP bar, even with an increase in diameter, is still lower than that of a high-yield threadbar of one size smaller. The different material properties indicate that larger deformation should occur in a GFRP soil-nail wall compared with a soil-nail wall reinforced with high-yield threadbar. No case studies could be found to prove this.*



**Figure 7** Double shear test on GFRP bar

shows the strength retention of CFRP and GFRP with the reduced tensile capacity. For a 100-year period the retention due to creep is 45% and 70% for GFRP and CFRP respectively.

To avoid failure of an FRP-reinforced member due to creep rupture, safe design stress levels below  $T_{ULS}$  should be maintained, and to prevent significant creep movements, safe stress levels less than  $T_{SLS}$  must be maintained. Table 1 already factored the short-term ultimate strengths of ASTEC bars accordingly. The equations below are simplifications of the ACI440 recommendations:

For the serviceability limit state, the following limits are applicable:

$$\begin{aligned} \text{GFRP: } T_{SLS} &= 0.2C_E f_{fu}^* \\ &= 0.2 \times 0.7 f_{fu}^* A \\ &= 0.14 f_{fu}^* A \end{aligned}$$

$$\begin{aligned} \text{CFRP: } T_{SLS} &= 0.55C_E f_{fu}^* \\ &= 0.55 \times 0.9 f_{fu}^* A \\ &= 0.495 f_{fu}^* A \end{aligned}$$

In the ultimate limit state, the following limits are applicable:

$$\begin{aligned} \text{GFRP: } T_{ULS} &= \phi C_E f_{fu}^* \\ &= 0.55 \times 0.7 f_{fu}^* A \\ &= 0.385 f_{fu}^* A \end{aligned}$$

$$\begin{aligned} \text{CFRP: } T_{ULS} &= \phi C_E f_{fu}^* \\ &= 0.55 \times 0.9 f_{fu}^* A \\ &= 0.495 f_{fu}^* A \end{aligned}$$

ASTEC GFRPs were tested in shear and performed well. The shear capacity increases significantly if the angle being tested at is smaller than  $90^\circ$  (Thomas 2019), as some of the shear load is transferred into a tensile load component. This shear capacity can be higher than that of steel. One should, however, also factor in this contribution to shear capacity with the applicable tensile factors provided in ACI440.

Shear capacity can be calculated empirically (Thomas 2019) or using actual test results. Testing is typically undertaken in accordance with ASTM D7617 and can be done with either a single shear test or a double shear test (Figure 7).

ASTEC recently undertook numerous tests on GFRP, with both vinylester and epoxy resin bars. The shear and moment capacity were also calculated in accordance with ACI440. These results are provided in Table 4.

*Shear capacity can be calculated empirically or using actual test results. Testing is typically undertaken in accordance with ASTM D7617 and can be done with either a single shear test or a double shear test.*

## BOND PERFORMANCE

Although the recommended formulae typically given for the design of soil nails and anchors assume that a uniform increased capacity can be achieved with an increase in fixed length, this is in fact not correct, as was already shown by Ostermayer in 1975 (Figure 8). This uniform increase can be reasonably assumed for short nails, typically  $<2.5$  m. For lengths exceeding 2.5 m the achieved bond strength between the soil and the grout body typically decreases with an increase in length; a significant increase in length results in only a small increase in capacity. For more elastic reinforcement, such as GFRP bars, the average bond strength achieved is lower than that for HTS. Figure 9 by Barley and Graham for London Clays (taken from *Bridges* 2015) shows that the stiffer (EA) the tendon, the more uniform the stress distribution along its length, and the more efficient the system is in increasing tensile resistance with an increase in fixed length. The guaranteed grout–GFRP bar bond strength for Dextra bars is 9 600 kPa.

**Table 4** Shear and moment capacity of ASTEC GFRP bars

GFRP bar	Unfactored ultimate 90° shear capacity assuming 150 MPa (kN)	Design ultimate bending moment capacity (kN.m)	SLS bending moment capacity (kN.m) (ACI440 (2015/2022))
19	42	0.23	0.09/0.135
25	73	0.525	0.19/0.285
32	120	1.113	0.40/0.60
41	198	2.34	0.84/1.26

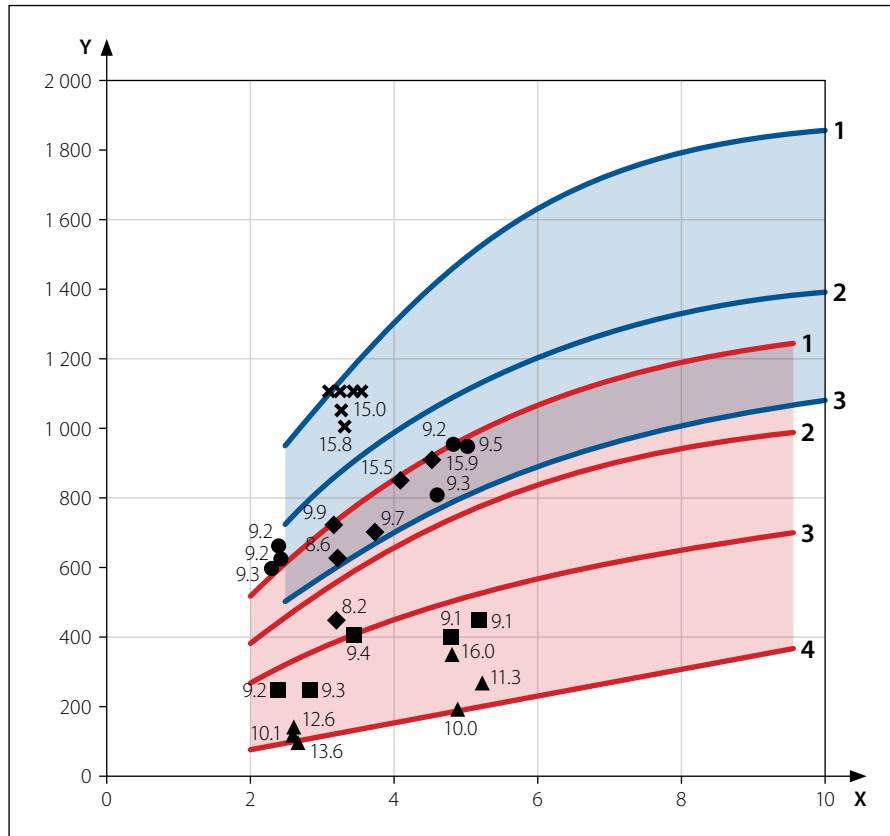


**Figure 8** Tensile capacity of fixed length (Y in kN) with a fixed length of X in m

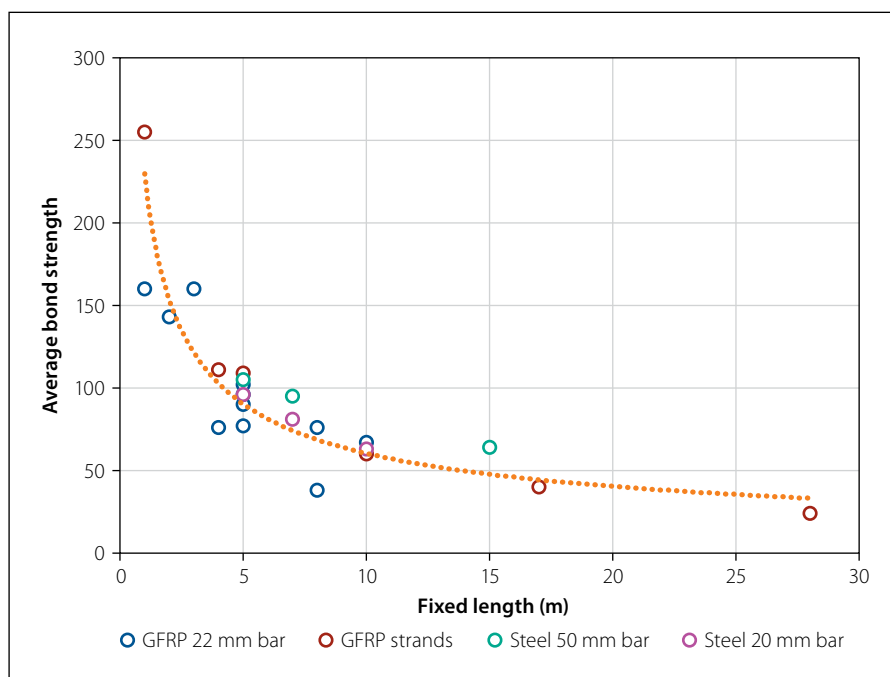


**Figure 9** Decrease in bond strength with an increase in fixed length (after Barley & Graham for London Clays, *Bridges* 2015)

It is, however, always recommended that the bond capacity be confirmed by undertaking pull-out tests, and that the above reduction with an increase in bond length be considered if testing short nails.

### INTERACTION AT THE FAILURE PLANE

Soil nails work predominately in tension, but due to relative displacement on the failure plane, shear forces will also develop in soil nails. These shear loads will induce a bending moment in the soil nail at a small distance inside the failure wedge and behind the failure plane, as shown in Figure 10. The behaviour is similar to that of a free-headed pile. These structural forces are normally not critical under serviceability conditions, as only small shear movements normally occur, but they could be problematic in the ultimate limit state. The mobilisation of shear forces and bending moments in soil nails is affected by the thickness of the shear zone. The wider the shear zone, the lower the shear forces and bending moments.

Conventionally for high-yield threadbar, this phenomenon can be reviewed using the equations provided in SANS 10162 for combined shear and tensile load, and for combined tensile load and bending moment, namely:

$$\frac{T_u}{T_r} + \frac{M_u}{M_r} \leq 1.0$$

and

$$\frac{T_u}{T_r} + \frac{V_u}{V_r} \leq 1.4$$

This phenomenon was assessed using both 2D and 3D geotechnical finite element software, modelling the nails as beam elements to ensure that shear forces and bending moments could develop.

The example consists of a 5 m soil-nail wall in a silty sandy material. A typical manual calculation will assume a redistribution of a triangular pressure for a

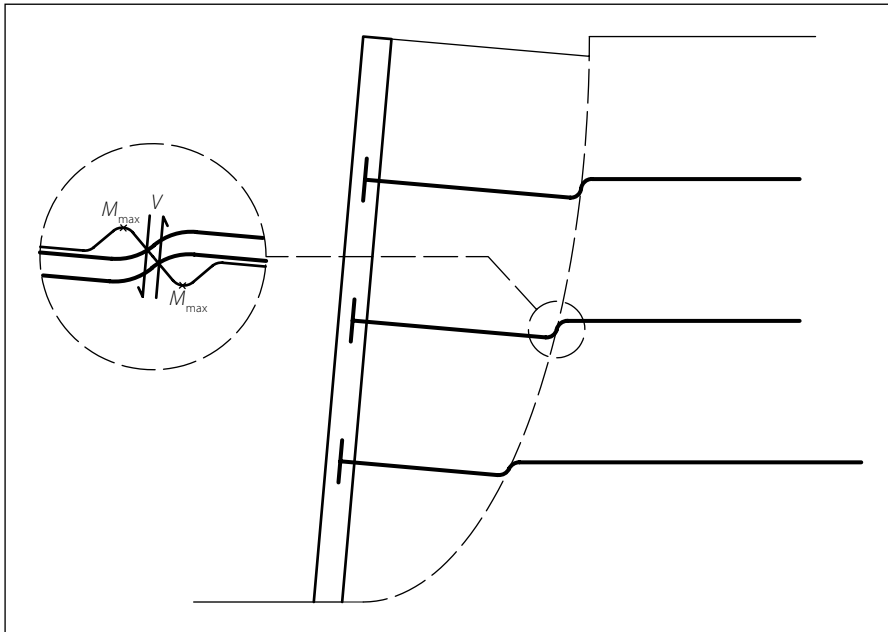


**Figure 10** Development of bending moment due to shear load intercept at failure plane

5 m high wall, i.e.  $0.5\gamma K_a H^2 sFoS = 0.5(18)(0.33)(5^2)1.5(1.5) = 167 \text{ kN}$ . For a three-nail vertical spacing, 55 kN ultimate capacity and 37 kN serviceability capacity would normally be designed for. According to ACI440 (2020), this would require the use of a GFRP bar of 19 mm governed by the SLS, and a 16 mm high-yield threadbar governed by the ULS in accordance with SANS 10162 (ignoring sacrificial thickness allowances) when considering tensile load only. In addition to the above calculation, it is assumed the excavation has sufficient “cohesion” to stand up vertically during excavation without support before the application of shotcrete and mesh, as described by Van der Merwe

and Schulz-Poblete (2019). Also, the nails need to be angled to intercept the failure plane at an angle larger than normal to ensure that tensile loads develop and that the nails do not go into compression. This will also ensure that bending moments in the soil nails are smaller.

The new guidelines on numerical modelling using EN1997 (2022+) were followed to assess the structural forces in the soil nails:

1. Input/Material Factoring Approach (MFA) using:

- factors of actions  $\gamma_F$  for GEO limit states
- factors on material properties  $\gamma_M$  from set EQU/GEO.

*The nails need to be angled to intercept the failure plane at an angle larger than normal to ensure that tensile loads develop and that the nails do not go into compression. This will also ensure that bending moments in the soil nails are smaller.*

There are two MFA checks, one where material properties are factored before all the stages from Stage 1, and the other after every stage to assess the structural forces.

2. Output/Effects Factoring Approach (EFA)

- factors of actions  $\gamma_E$  and effects-of-action  $\gamma_E$  for STR-P limit states as given in SANS 10160-1
- factors on material properties  $\gamma_M$  from set STR/STR-P.

The soil nails were modelled in a staged excavation in RS2 and RS3 (Rocscience 2019), as shown in Figures 11(a) and 11(b).

Table 5 summarises the structural forces derived in the nails from the FE analysis, assuming the bending stiffness with an uncracked grout body.

It can be seen from the structural forces in Table 5 that the shear forces are small, contrary to what was believed, but that large moments (relative to the bars’ moment capacities) develop. Therefore the nail should be sized as follows to prevent

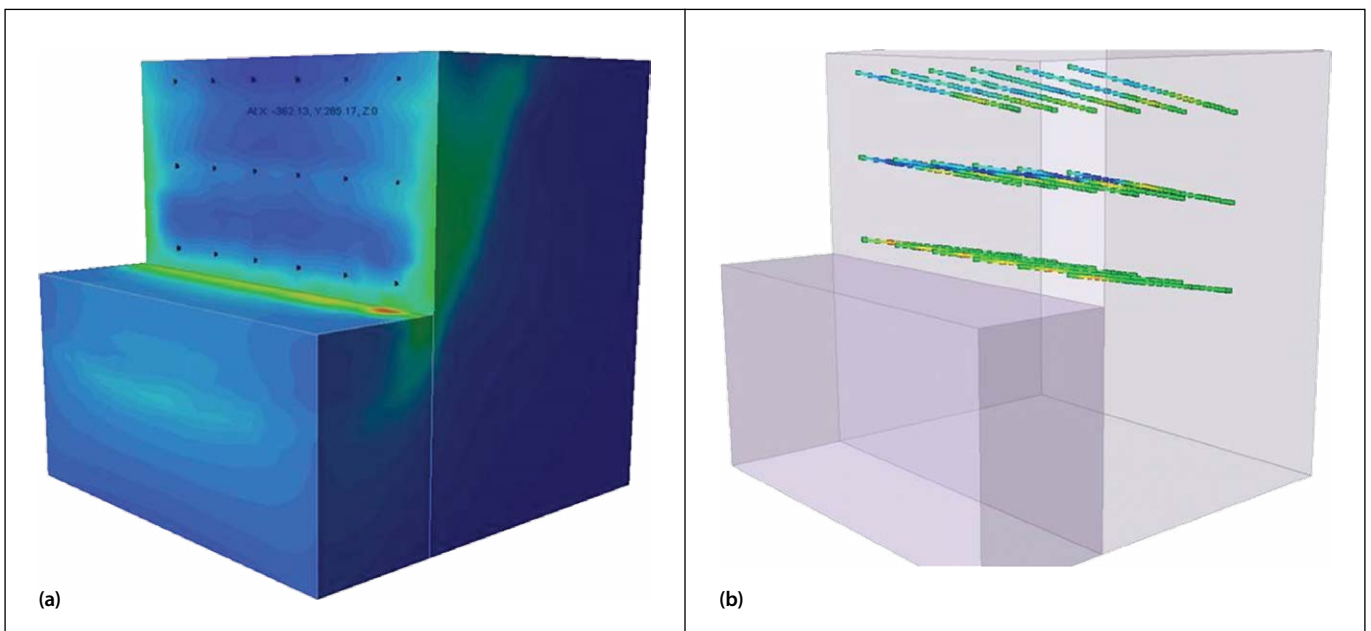


**Figure 11** (a) RS2 model of soil nail wall example and (b) RS3 model of soil nail wall example

exceeding the SLS or ULS stress limits in the fibres furthest from the neutral axis (ignoring tensile and compressive capacity from the grout body):

$$\sigma_{\text{uls or } \sigma_{\text{sls}}} > \frac{T}{A} + \frac{My}{I}$$

where  $\sigma_{\text{uls}}$  or  $\sigma_{\text{sls}}$  is the design ultimate tensile load or the working tensile load divided by the cross-sectional area respectively.

This check is undertaken as follows:

$$\frac{239}{\left[\frac{32}{2000}\right]^2 \pi} > \frac{77}{\left[\frac{32}{2000}\right]^2 \pi} + \frac{0.27 \left[\frac{32}{2000}\right]}{\pi \left[\frac{32}{1000}\right]^4} \frac{1}{64}$$

a 32 mm GFRP bar in the ULS.

For the SLS:

$$\frac{88}{\left[\frac{32}{2000}\right]^2 \pi} > \frac{31}{\left[\frac{32}{2000}\right]^2 \pi} + \frac{0.19 \left[\frac{32}{2000}\right]}{\pi \left[\frac{32}{1000}\right]^4} \frac{1}{64}$$

a 32 mm GFRP bar is required using ACI440 (2022) recommendations.

For an equivalent high-yield threadbar, and allowing for sacrificial thickness, the ULS will require the use of a 25 mm bar. Under the above SLS loading conditions the grout section will, however, crack due to the large tensile stresses that develop in the grout body, and perhaps the structural properties (EA and EI) of only the GFRP bar should be used as input in the FE model.

**Table 5** Nail forces from EFA, MFA (from first stage) and MFA (after every stage)

Method	Axial (kN)	Shear force (kN)	Bending moment (kN.m)
EFA (unfactored SLS)	31.5	0.18	0.19
EFA (factored by 1.35)	42.5	0.25	0.26
MFA (all stages factored)	77	0.3	0.27
MFA (final stage factored)	69	1.2	0.225

Therefore, when a cracked grout body is assumed (as by Shiu & Chang 2005), and assuming only the bending stiffness of the bar in the FE analysis, the diameters can be decreased by one size for high-yield threadbar and two sizes for GFRP due to the reduced bending moments developing in the GFRP soil nails. Large shearbox test studies with GFRP soil nails would prove valuable in assessing the behaviour of more brittle GFRP soil nails.

### COST COMPARISON

When a high-yield threadbar is compared with a GFRP bar of the same diameter, the cost of the GFRP will be 1 to 1.5 times the cost of the high-yield threadbar, depending on the number of couplers required. However, when allowance is made for DCP HDPE sheathing to protect the high-yield threadbar from corrosion, the GFRP bar will become more economical. CFRP typically costs two to three times the price of a comparable GFRP bar.

### CONCLUSIONS

GFRP soil nails and CFRP stressed anchors are recognised technology with excellent durability for design lives

exceeding 100 years. The long-term creep properties of GFRP and CFRP significantly affect the design working loads of these elements and eliminate the requirement for double corrosion protection. Although the contribution of the bending moment and shear capacity of soil nails is typically ignored in the design of conventional soil nails, it is recommended that these structural forces should be assessed and the element designed accordingly to ensure that brittle nail failures do not occur. Typically, a GFRP bar, for Dextra products, of one diameter larger needs to be used in comparison with a conventional high-yield threadbar solution, as shown in this study. Pull-out resistance might be lower than for conventional soil nails and needs to be tested to ensure that there is sufficient length behind the failure plane. The costs of these GFRP bars should be comparable to those of high-yield threadbar when the need for DCP sheathing is eliminated.

### NOTE

Reference details are available from the authors. □

# Invitation to all history-minded SAICE members 50<sup>th</sup> Anniversary of the Orange River Project

The Orange River Project was one the largest water projects ever undertaken in South Africa.

To commemorate the 50<sup>th</sup> anniversary of the completion of this major project, the SAICE History and Heritage Panel and SAICE Water Division are planning to release a commemorative booklet. It will probably be in A4 softcover format, similar to the Water Division's 50<sup>th</sup> anniversary booklet of a few years ago.

As the technical aspects of the project have already been covered in detail over many years, the intention is to concentrate more on the reminiscences and experiences of people who worked on the project.

The writing of the booklet is still in the preliminary phase, and we are looking for people who would like to contribute or become involved. Debbie Besseling, who acts as administrator for a number of the SAICE Divisions, has agreed to help with editing the content.

Anyone who is interested in contributing or becoming involved should please contact Chris Roth, chairman of the History and Heritage Panel, at the following address:  
[chris.roth@up.ac.za](mailto:chris.roth@up.ac.za)

We look forward to hearing from you! □